

Full-length transcriptome assembly from RNA-Seq data without a reference genome

Manfred G Grabherr^{1,8}, Brian J Haas^{1,8}, Moran Yassour^{1–3,8}, Joshua Z Levin¹, Dawn A Thompson¹, Ido Amit¹, Xian Adiconis¹, Lin Fan¹, Rakim Raychowdhury¹, Qiandong Zeng¹, Zehua Chen¹, Evan Mauceli¹, Nir Hacohen¹, Andreas Gnirke¹, Nicholas Rhind⁴, Federica di Palma¹, Bruce W Birren¹, Chad Nusbaum¹, Kerstin Lindblad-Toh^{1,5}, Nir Friedman^{2,6} & Aviv Regev^{1,3,7}

Massively parallel sequencing of cDNA has enabled deep and efficient probing of transcriptomes. Current approaches for transcript reconstruction from such data often rely on aligning reads to a reference genome, and are thus unsuitable for samples with a partial or missing reference genome. Here we present the Trinity method for *de novo* assembly of full-length transcripts and evaluate it on samples from fission yeast, mouse and whitefly, whose reference genome is not yet available. By efficiently constructing and analyzing sets of de Bruijn graphs, Trinity fully reconstructs a large fraction of transcripts, including alternatively spliced isoforms and transcripts from recently duplicated genes. Compared with other *de novo* transcriptome assemblers, Trinity recovers more full-length transcripts across a broad range of expression levels, with a sensitivity similar to methods that rely on genome alignments. Our approach provides a unified solution for transcriptome reconstruction in any sample, especially in the absence of a reference genome.

Recent advances in massively parallel cDNA sequencing (RNA-Seq) provide a cost-effective way to obtain large amounts of transcriptome data from many organisms and tissue types^{1,2}. In principle, such data can allow us to identify all expressed transcripts³, as complete and contiguous mRNA sequence from the transcription start site to the transcription end, for multiple alternatively spliced isoforms. However, reconstruction of all full-length transcripts from short reads with considerable sequencing error rates poses substantial computational challenges⁴: (i) some transcripts have low coverage, whereas others are highly expressed; (ii) read coverage may be uneven across the transcript's length, owing to sequencing biases; (iii) reads with sequencing errors derived from a highly expressed transcript may be more abundant than correct reads from a transcript that is not highly expressed; (iv) transcripts encoded by adjacent loci can overlap and thus can be erroneously fused to form a chimeric transcript; (v) data structures need to accommodate multiple transcripts per locus, owing to alternative splicing; and (vi) sequences that are repeated in different genes introduce ambiguity. A successful method should address each challenge, be applicable to both complex mammalian genomes and gene-dense microbial genomes, and be able to reconstruct transcripts of variable sizes, expression levels and protein-coding capacity.

There are two alternative computational strategies for transcriptome reconstruction⁴. Mapping-first approaches⁵, such as Scripture³ and Cufflinks², first align all the reads to a reference (unannotated) genome

and then merge sequences with overlapping alignment, spanning splice junctions with reads and paired-ends. Assembly-first (*de novo*) methods, such as ABySS¹, SOAPdenovo⁶ or Oases (E. Birney, European Bioinformatics Institute, personal communication), use the reads to assemble transcripts directly, which can be mapped subsequently to a reference genome, if available. Mapping-first approaches promise, in principle, maximum sensitivity, but depend on correct read-to-reference alignment, a task that is complicated by splicing, sequencing errors and the lack or incompleteness of many reference genomes. Conversely, assembly-first approaches do not require any read-reference alignments, important when the genomic sequence is not available, is gapped, highly fragmented or substantially altered, as in cancer cells.

Successful mapping-first methods were developed in the past year⁴, but substantially less progress was made to date in developing effective assembly-first approaches. As the number of reads grows, it is increasingly difficult to determine which reads should be joined into contiguous sequence contigs. An elegant computational solution is provided by the de Bruijn graph^{7,8}, the basis for several whole-genome assembly programs^{9–11}. In this graph, a node is defined by a sequence of a fixed length of k nucleotides (' k -mer', with k considerably shorter than the read length), and nodes are connected by edges, if they perfectly overlap by $k - 1$ nucleotides, and the sequence data support this connection. This compact representation allows for enumerating all possible solutions by which linear sequences can be reconstructed given overlaps of $k - 1$.

¹Broad Institute of Massachusetts Institute of Technology and Harvard, Cambridge, Massachusetts, USA. ²School of Computer Science, Hebrew University, Jerusalem, Israel. ³Department of Biology, Massachusetts Institute of Technology, Cambridge, Massachusetts, USA. ⁴Department of Biochemistry and Molecular Pharmacology, University of Massachusetts Medical School, Worcester, Massachusetts, USA. ⁵Science for Life Laboratory, Department of Medical Biochemistry and Microbiology, Uppsala University, Uppsala, Sweden. ⁶Alexander Silberman Institute of Life Sciences, Hebrew University, Jerusalem, Israel. ⁷Howard Hughes Medical Institute, Department of Biology, Massachusetts Institute of Technology, Cambridge, Massachusetts, USA. ⁸These authors contributed equally to this work. Correspondence should be addressed to N.F. (nir@cs.huji.ac.il) or A.R. (aregev@broad.mit.edu).

Received 3 December 2010; accepted 28 April 2011; published online 15 May 2011; doi:10.1038/nbt.1883

For transcriptome assembly, each path in the graph represents a possible transcript. A scoring scheme applied to the graph structure can rely on the original read sequences and mate-pair information to discard non-sensical solutions (transcripts) and compute all plausible ones.

Applying the scheme of de Bruijn graphs to *de novo* assembly of RNA-Seq data represents three critical challenges: (i) efficiently constructing this graph from large amounts (billions of base pairs) of raw data; (ii) defining a suitable scoring and enumeration algorithm to recover all plausible splice forms and paralogous transcripts; and (iii) providing robustness to the noise stemming from sequencing errors and other artifacts in the data. In particular, sequencing errors would introduce a large number of false nodes, resulting in a massive graph with millions of possible (albeit mostly implausible) paths.

Here, we present Trinity, a method for the efficient and robust *de novo* reconstruction of transcriptomes, consisting of three software modules: Inchworm, Chrysalis and Butterfly, applied sequentially to process large volumes of RNA-Seq reads. We evaluated Trinity on data from two well-annotated species—one microorganism (fission yeast) and one mammal (mouse)—as well as an insect (the whitefly *Bemisia tabaci*), whose genome has not yet been sequenced. In each case, Trinity recovers most of the reference (annotated) expressed transcripts as full-length sequences, and resolves alternative isoforms and duplicated genes, performing better than other available transcriptome *de novo* assembly tools, and similarly to methods relying on genome alignments.

RESULTS

Trinity: a method for *de novo* transcriptome assembly

In contrast to *de novo* assembly of a genome, where few large connected sequence graphs can represent connectivities among reads across entire chromosomes, in assembling transcriptome data we expect to encounter numerous individual disconnected graphs, each representing the transcriptional complexity at nonoverlapping loci. Accordingly, Trinity partitions the sequence data into these many individual graphs, and then processes each graph independently to extract full-length isoforms and tease apart transcripts derived from paralogous genes.

In the first step in Trinity, Inchworm assembles reads into the unique sequences of transcripts. Inchworm (Fig. 1a) uses a greedy *k*-mer-based approach for fast and efficient transcript assembly, recovering only a single (best) representative for a set of alternative variants that share *k*-mers (owing to alternative splicing, gene duplication or allelic variation). Next, Chrysalis (Fig. 1b) clusters related contigs that correspond to portions of alternatively spliced transcripts or otherwise unique portions of paralogous genes. Chrysalis then constructs a de Bruijn graph for each cluster of related contigs, each graph reflecting the

complexity of overlaps between variants. Finally, Butterfly (Fig. 1c) analyzes the paths taken by reads and read pairings in the context of the corresponding de Bruijn graph and reports all plausible transcript sequences, resolving alternatively spliced isoforms and transcripts derived from paralogous genes. Below, we describe each of Trinity's modules.

Inchworm assembles contigs greedily and efficiently

Inchworm efficiently reconstructs linear transcript contigs in six steps (Fig. 1a). Inchworm (i) constructs a *k*-mer dictionary from all sequence reads (in practice, *k* = 25); (ii) removes likely error-containing *k*-mers from the *k*-mer dictionary; (iii) selects the most frequent *k*-mer in the dictionary to seed a contig assembly, excluding both low-complexity

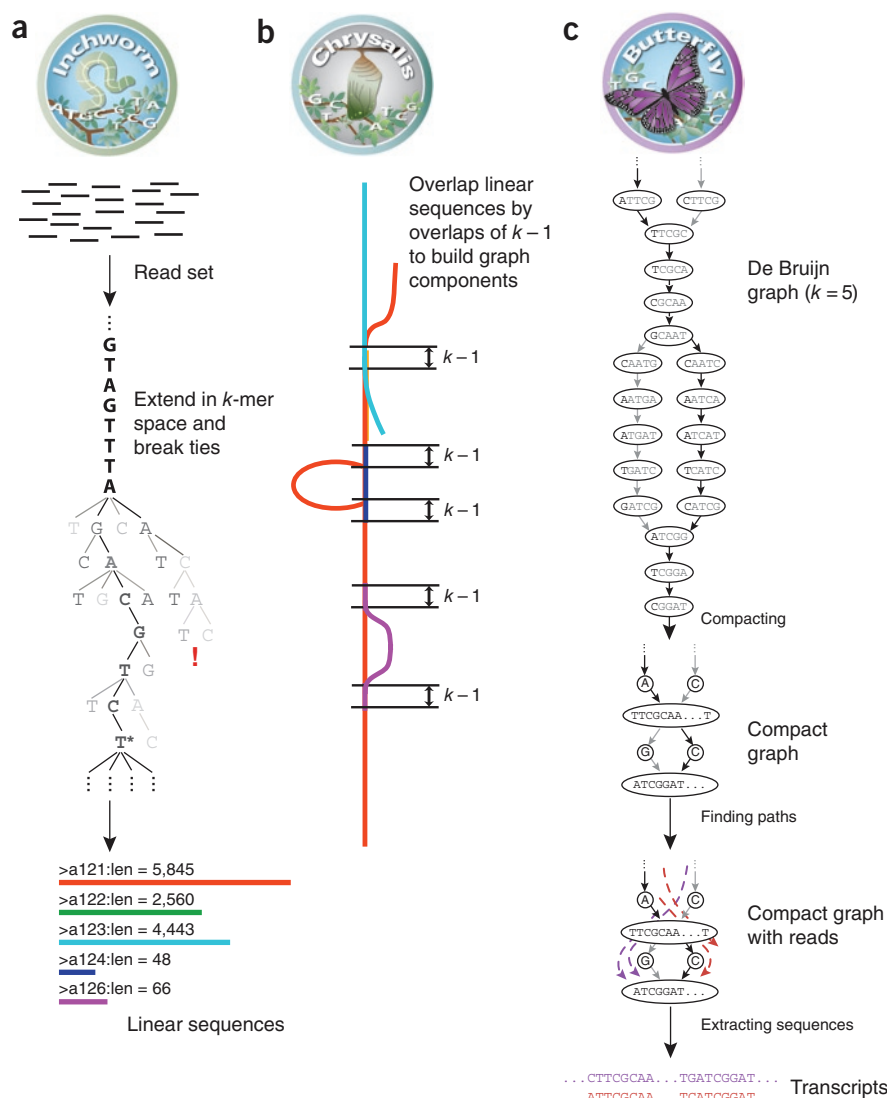


Figure 1 Overview of Trinity. (a) Inchworm assembles the read data set (short black lines, top) by greedily searching for paths in a *k*-mer graph (middle), resulting in a collection of linear contigs (color lines, bottom), with each *k*-mer present only once in the contigs. (b) Chrysalis pools contigs (colored lines) if they share at least one *k* – 1-mer and if reads span the junction between contigs, and then it builds individual de Bruijn graphs from each pool. (c) Butterfly takes each de Bruijn graph from Chrysalis (top), and trims spurious edges and compacts linear paths (middle). It then reconciles the graph with reads (dashed colored arrows, bottom) and pairs (not shown), and outputs one linear sequence for each splice form and/or paralogous transcript represented in the graph (bottom, colored sequences).

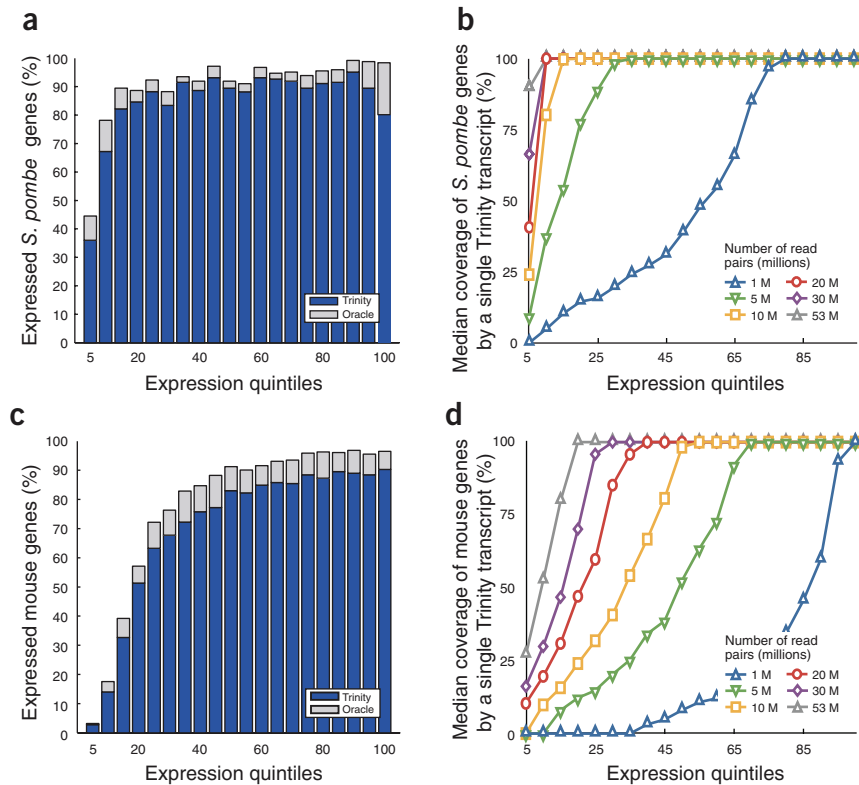
Figure 2 Trinity correctly reconstructs the majority of full-length transcripts in fission yeast and mouse. **(a,c)** The fraction of genes that are fully reconstructed and in the Oracle Set in different expression quintiles (5% increments) in fission yeast (50 M pairs assembly) (**a**) and the fraction of genes that have at least one fully reconstructed transcript and are in the Oracle Set in different expression quintiles in mouse (53 M pairs assembly) (**c**). Each bar represents a 5% quintile of read coverage for genes expressed. Gray bars show the remaining fraction of transcripts that are in the Oracle Set but not fully reconstructed. For example, ~36% of the *S. pombe* transcripts at the bottom 5% of expression levels are fully reconstructed by Trinity; ~45% of the transcripts in this quintile are in the Oracle Set. **(b,d)** Curves show the median values for coverage (as fraction of length of reference transcripts) by the longest corresponding Trinity-assembled transcript, according to expression quintiles in yeast (**b**) and mouse (**d**), depending on the number of read pairs that went into each assembly.

and singleton k -mers (appearing only once); (iv) extends the seed in each direction by finding the highest occurring k -mer with a $k - 1$ overlap with the current contig terminus and concatenating its terminal base to the growing contig sequence (once a k -mer has been used for extension, it is removed from the dictionary); (v) extends the sequence in either direction until it cannot be extended further, then reports the linear contig; (vi) repeats steps iii–v, starting with the next most abundant k -mer, until the entire k -mer dictionary has been exhausted.

The contigs reported by Inchworm alone do not capture the full complexity of the transcriptome; for example, only one alternatively spliced variant can be reported at full length per locus, with partial sequences reported for unique regions of any alternatively spliced transcripts. However, its contigs do maintain the information required by subsequent Trinity components to reconstruct and search the entire graph containing all possible sequences. Indeed, except for low-complexity and singleton k -mers excluded from seeds or discarded in contigs shorter than the minimum length required, Inchworm's contigs provide a complete representation of the sequence overlap-based de Bruijn graph, with each k -mer being unique in the set, and the $k - 1$ subsequences implicitly defining the edges in the graph. This approach is much more efficient than computing a full graph from all reads at once, and it quickly provides a meaningful intermediate output of the contigs strongly supported by many k -mers in the reads. By eliminating singleton k -mers as initial seeds for contig extensions, Inchworm further reduces the inclusion in assemblies of k -mers likely resulting from sequencing errors.

Chrysalis builds de Bruijn transcript graphs

Chrysalis clusters minimally overlapping Inchworm contigs into sets of connected components, and constructs complete de Bruijn graphs for each component (Fig. 1b). Each component defines a collection of Inchworm contigs that are likely to be derived from alternative splice forms or closely related paralogs. Chrysalis works in three phases. (i) It recursively groups Inchworm contigs into connected components. Contigs are grouped if there is a perfect overlap of $k - 1$ bases between them and if there is a minimal number of reads that span the junction



across both contigs with a $(k - 1)/2$ base match on each side of the $(k - 1)$ -mer junction. (ii) It builds a de Bruijn graph for each component using a word size of $k - 1$ to represent nodes, and k to define the edges connecting the nodes. It weights each edge of the de Bruijn graph with the number of k -mers in the original read set that support it. (iii) It assigns each read to the component with which it shares the largest number of k -mers, and determines the regions within each read that contribute k -mers to the component.

Butterfly resolves alternatively spliced and paralogous transcripts

Butterfly reconstructs plausible, full-length, linear transcripts by reconciling the individual de Bruijn graphs generated by Chrysalis with the original reads and paired ends. It reconstructs distinct transcripts for splice isoforms and paralogous genes, and resolves ambiguities stemming from errors or from sequences $>k$ bases long that are shared between transcripts.

Butterfly consists of two parts (Fig. 1c). During the first part, called graph simplification, Butterfly iterates between (i) merging consecutive nodes in linear paths in the de Bruijn graph to form nodes that represent longer sequences and (ii) pruning edges that represent minor deviations (supported by comparatively few reads), which likely correspond to sequencing errors. Diploid polymorphisms are expected to be more frequent than sequencing errors and will likely be maintained. In the second part, called plausible path scoring, Butterfly identifies those paths that are supported by actual reads and read pairs, using a dynamic programming procedure that traverses potential paths in the graph while maintaining the reads (and pairs) that support them. Because reads and sequence fragments (paired reads) are typically much longer than k , they can resolve ambiguities and reduce the combinatorial number of paths to a much smaller number of actual transcripts, enumerated as linear sequences.

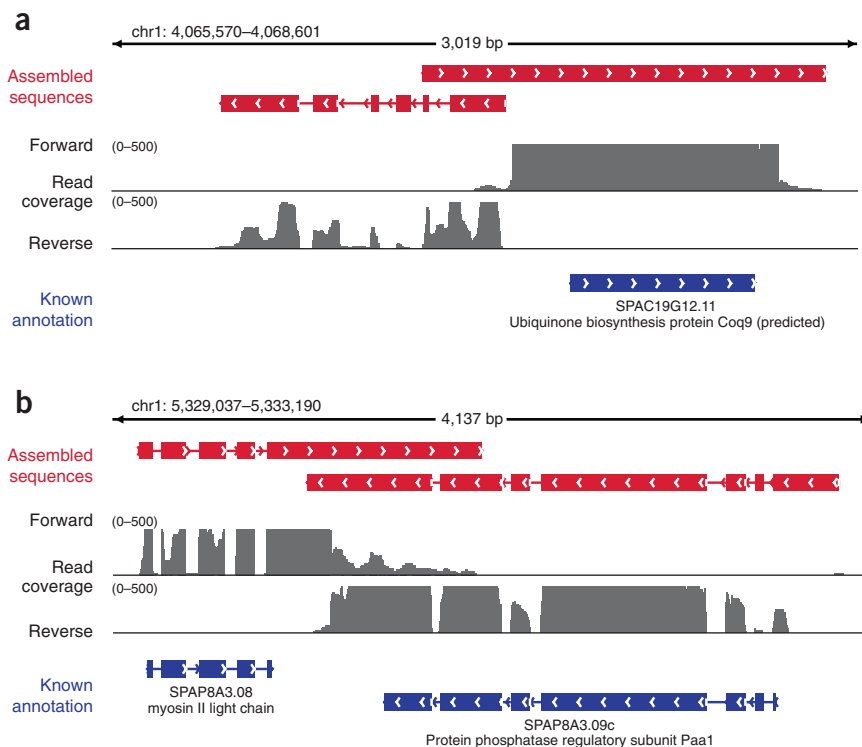


Figure 3 Trinity improves the yeast annotation. Shown are examples of Trinity assemblies (red) along with the corresponding annotated transcripts (blue) and underlying reads (gray) all aligned to the *S. pombe* genome (read alignment is shown for graphical clarity; no alignments were used to generate the assemblies). **(a)** Trinity identifies a new multi-exonic transcript (left) and extends the 5' and 3' UTRs of the *coq9* gene (right). **(b)** Trinity extends the UTRs of two convergently transcribed and overlapping genes.

RNA-Seq of *Schizosaccharomyces pombe*

We first generated RNA-Seq data from the fission yeast *S. pombe*. The *S. pombe* transcriptome¹² has relatively substantial splicing for a eukaryotic microorganism, with short introns (mean intron length = 80.6 bp) and dense transcripts (mean intergenic region = 938 bp based on coding genes only). To maximize transcript coverage, we pooled ~154 million pairs of strand-specific^{13,14}, 76-base Illumina read sequences from four biological conditions: mid-log growth, growth after all glucose has been consumed, late stationary phase and heat shock¹⁵.

Sensitivity limit for full-length reconstruction

We next estimated the upper sensitivity limit for which annotated transcripts can possibly be perfectly reconstructed given a particular data set of sequences. Any assembly approach based on a particular *k*-length oligomer is limited to those sequences that are represented by the exact *k*-mer composition of the RNA-Seq read set. To determine this empirical upper sensitivity limit, we built a *k*-mer dictionary from all the reads and identified all known reference protein-coding sequences that are reconstructable to full length given the read set, as those sequences that can be populated by adjacent and overlapping *k*-mers across their entire length. We call this set of sequences the 'Oracle Set'. Because this set also contains transcript sequences that are covered by *k*-mers, but not entire reads, some transcripts will appear reconstructable but are not. Conversely, the Oracle Set reflects only annotated known genes and known isoforms, which are likely an underestimate, especially in mammals¹⁶. Nevertheless, the Oracle Set provides a useful sensitivity benchmark.

In the *S. pombe* data set, nearly all (91%, 4,600/5,064) reference protein-coding sequences exist in the Oracle Set (25-mer dictionary, 154 M paired-reads), as almost all encoded transcripts (98%) are expressed in the measured conditions (≥ 0.5 fragments per transcript kilobase per million fragments mapped (FPKM)), consistent with previous studies in yeasts^{5,17,18}. When reducing the coverage by random sub-sampling, the size of the Oracle Set is saturated at 50 M paired reads (4,494/5,064, Supplementary Fig. 1), which we chose as our subsequent benchmarking set.

Trinity recovered most *S. pombe* transcripts

From the 50 M pairs of reads, Trinity fully reconstructed 86% of annotated transcripts (4,338/5,064, Supplementary Table 1) at full length, including 94% of the stringently defined oracle transcripts (4,218/4,494). Of the 276 oracle transcripts not fully reconstructed, 90 (33%) are reconstructed over at least 90% of their length, and 177 (64%) are reconstructed over at least 50% of their length.

Overall, Trinity generated 27,841 linear contigs longer than 100 bases, grouped into 23,232 components (Supplementary Note). Only 2,454 of the 27,841 Trinity contigs did not align to the genome using GMAP¹⁹. Of those, 30% match a UniRef90 (ref. 20) protein (BLASTX E $\leq 10^{-10}$), almost invariably (90%) a *Schizosaccharomyces* protein, and likely reflect assemblies with error-rich reads.

Trinity reconstructs full-length transcripts across a broad range of expression levels and sequencing depths (Fig. 2). For example, it accurately captured the full-length transcript of 71% of genes from the second quintile (5–10%), and had full-length coverage of 81–95% of annotated transcripts in the remaining quintiles (Fig. 2a). Considering both full-length and partial reconstructions, Trinity reconstructed a large fraction of the bases in each transcript (Fig. 2b).

In many cases, Trinity accurately resolved the sequences of closely related paralogous transcripts. Out of 77 gene families containing 185 paralogs²¹, Trinity recovered at full length all members of 33 families (68 genes), at least one member from an additional 33 families (46 genes found, 45 genes missing), and missed all 26 genes in the remaining 11 families, often involving genes not highly expressed. Some of the most highly expressed transcripts in *S. pombe* are derived from paralogous genes with very similar sequences (e.g., those encoding ribosomal proteins²¹), yet were resolved by Trinity.

Extended UTRs and long anti-sense transcripts in *S. pombe*

Compared to the existing annotation, Trinity extended the 5' untranslated region (UTR) of 312 transcripts (median extension, 80 bp; average, 176 bp), and the 3' UTR of 543 transcripts (median, 72 bp; average, 172 bp) (Supplementary Fig. 2a,b). It also found 3,726 previously unannotated 5' UTRs (median length, 183 bp; average length, 288 bp), and 3,416 3' UTRs (median length, 272 bp; average length, 397 bp).

Trinity identified 2,319 transcripts at 1,235 intergenic loci as novel transcribed sequences (Fig. 3a) and 612 long antisense transcripts that covered >75% of the length of the corresponding sense

Figure 4 Trinity resolves closely paralogous genes. (a) The compacted component graph for two paralogous mouse genes, *Ddx19a* and *Ddx19b* (93% identity). Red and blue arrows highlight the two paths chosen by Trinity out of the 64 possible paths in this portion of the graph alone. Numbers on the edges indicate the number of supporting reads; numbers in parentheses represent the sequence length at each node. (b) Alignments between the transcripts represented by the red and blue paths in a and the paralogous genes *Ddx19a* and *Ddx19b* relative to the mouse reference genome (genome alignment shown for graphical clarity only; no alignments were used to generate the assemblies).

transcript (Fig. 3b), and were not likely to be derived from extended transcription of a neighboring gene. One hundred thirteen of the intergenic transcripts and 612 long antisense transcripts were multiexonic. Although both were expressed at lower levels on average than annotated protein-coding genes (Supplementary Fig. 3), 49 long antisense transcripts (at 35 loci) were at least fivefold more highly expressed than the corresponding sense coding transcript (e.g., an antisense transcript to the meiotic gene *mug27/slk1* (SPCC417.06c) was >100-fold more highly expressed, Supplementary Fig. 4). This supports a role for antisense transcriptional regulation in meiosis for *S. pombe*^{15,22–24}, and is consistent with previous findings in *S. cerevisiae*²⁵.

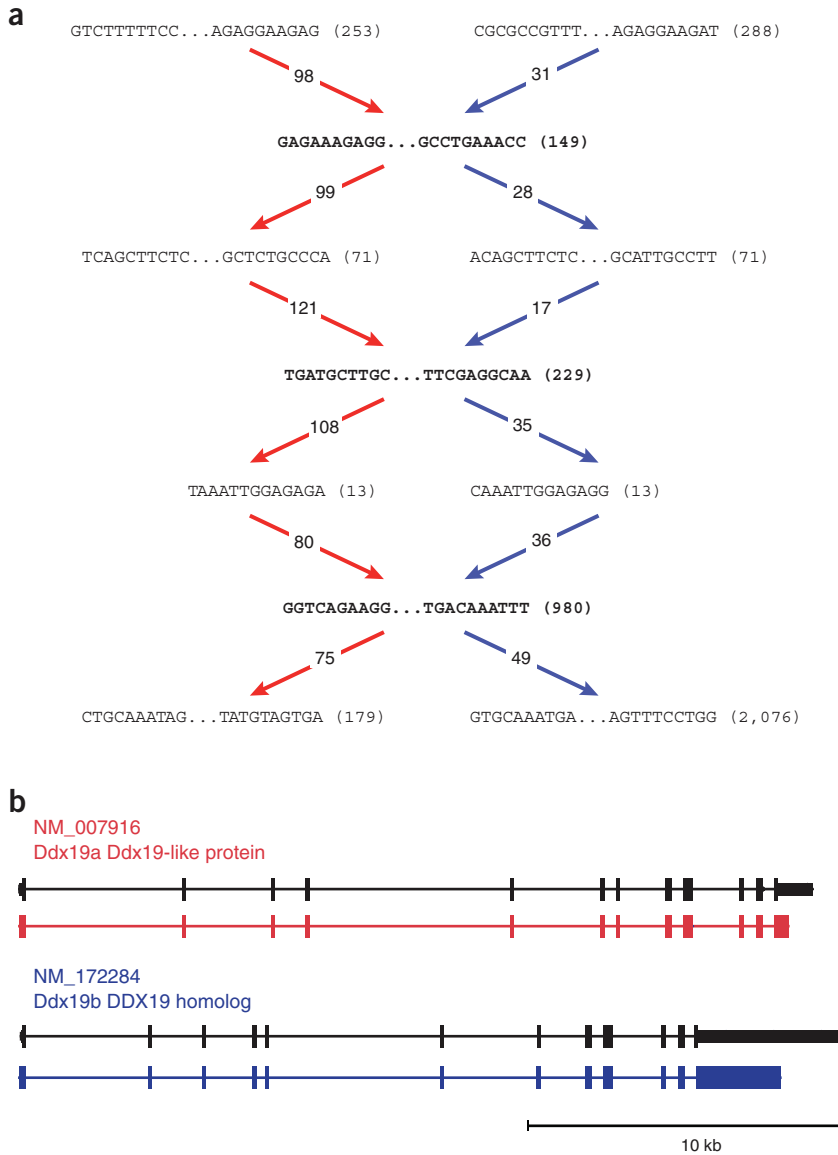
Trinity recovered most expressed annotated mouse transcripts

Compared to yeasts, mammalian transcriptomes exhibit substantially more complex patterns of alternative splicing²⁶. To test Trinity's ability to identify different isoforms, we sequenced ~52.6 million 76-base read pairs from C567BL/6 mouse primary immune dendritic cells. Unlike in *S. pombe*, only 54% of known mouse genes (10,724) were identified as expressed (≥ 0.5 FPKM), and of those, the Oracle Set determined 8,358 to be full-length reconstructable (727 loci have two or more isoforms variable in the protein-coding sequences, totaling 9,258 transcripts).

Trinity reported 48,497 contigs longer than 350 bp, capturing 8,185 transcripts to full-length (Supplementary Table 2 and Supplementary Note), corresponding to 7,749 loci (including 7,947 (86%) transcripts at 7,573 (91%) loci in the mouse Oracle Set). The percentage of transcripts recovered to full-length and the fraction of length captured were high across a broad range of expression levels (Fig. 2c,d).

Trinity resolved splice isoforms and gene paralogs in a manner consistent with the mouse Oracle Set. Trinity found 872 full-length, alternatively spliced, isoforms from 385 loci (53% of the loci with alternatively spliced variants in the Oracle Set), and matched the full-length transcripts for 463 (61.6%) of 752 paralogous transcripts in the Oracle Set (>70% identity between paralogs, Fig. 4).

Trinity extended the annotated 5' UTR for 5,265 transcripts (5,036 loci, median length, 43; average length, 91, Supplementary Fig. 2c), and included one or more additional 5' UTR exons in 305 cases



(Supplementary Fig. 5). It extended the 3' UTR in 2,918 transcripts (2,819 loci, median length, 20; average length, 248; Supplementary Fig. 2d), adding 3' UTR exons in 62 cases (Supplementary Fig. 2b). Differences in UTR length were often due to alternative splicing events restricted to the UTR.

High sequence fidelity of reconstructed transcripts

We measured the assembled transcript base error rate by aligning the full-length transcripts to the corresponding reference genome (using BLAT), and capturing mismatches, insertions and deletions from the highest scoring alignment (Supplementary Table 3). In fission yeast, rates of mismatches, insertions and deletions are each <1 in 10,000. In mouse, rates were approximately twice as high, reflecting the lower transcript fold-coverage. As the raw read error rate is ~1%, Trinity thus resolved ~99% of sequencing errors.

Comparing Trinity's performance to other methods

We compared Trinity's performance to that of other assemblers by several measures. First, we examined the number of reference transcripts reconstructed to full-length by each method ('sensitivity'). In *S. pombe*, Trinity

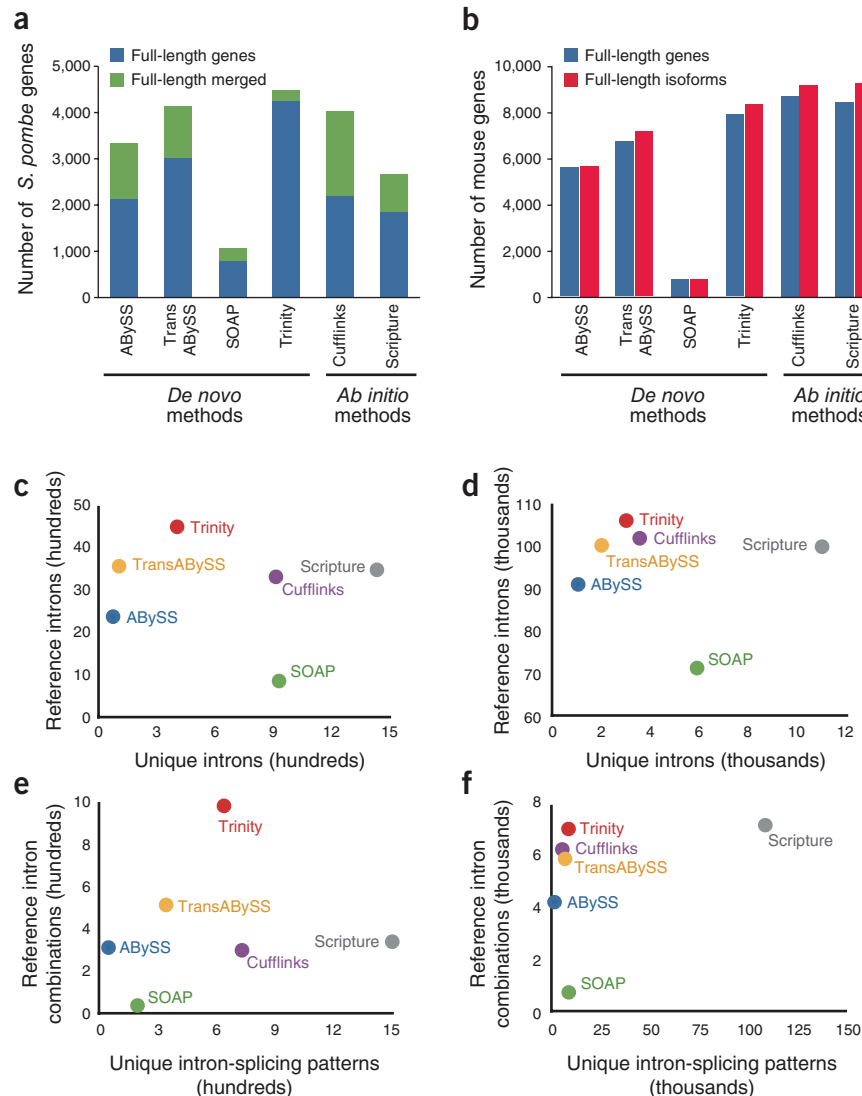


Figure 5 Comparison of Trinity to other mapping-first and assembly-first methods. **(a,b)** Evaluation based on number of full-length annotated transcripts reconstructed by each method in *S. pombe* (50 M read pair assemblies) **(a)** and mouse (53 M read pair assemblies) **(b)**. Number of genes reconstructed in full length (blue) or as fusions of two full-length genes (green, yeast only) and the number of full-length reconstructed transcript isoforms (red, mouse only) in each of four assembly-first (*de novo*) and two mapping-first approaches. **(c,d)** Evaluation based on the number of introns defined by the transcripts from each method for *S. pombe* **(c)** and mouse **(d)**. Shown is the number of distinct introns consistent with the reference annotation (y axis) versus the number of uniquely predicted introns (x axis), based on mapping to the genome of the transcripts reconstructed by the different methods. **(e,f)** Evaluation based on the number of splicing patterns (complete sets of introns in multi-intronic transcripts) defined by the transcripts from each method for *S. pombe* **(e)** and mouse **(f)**. Shown are the numbers of distinct splicing patterns (y axis) consistent with the reference annotation versus the number of unique splicing patterns (x axis), for each method.

outperformed the *de novo* sequence assemblers, ABYSS¹, Trans-ABYSS²⁷ and SOAPdenovo⁶, as well as the mapping-first programs Scripture³ and Cufflinks² (Fig. 5a). Trinity performed well across a range of 10 M to the full 150 M input sequence reads, whereas the alternative methods tended to peak at ~50 M pairs or smaller inputs (Supplementary Fig. 6a). In mouse (Ref-Seq annotation set, Fig. 5b), Trinity (8,185 transcripts; 7,749 genes) outperformed the other *de novo* assembly methods ABYSS (5,561; 5,500), Trans-ABYSS (7,025; 6,598) and SOAPdenovo (761; 760), with the mapping-first programs Cufflinks (9,010; 8,536) and Scripture (9,086;

8,293) exhibiting better sensitivity. Furthermore, Trinity and Cufflinks appear best-tuned in their sensitivity across the broadest range of expression levels (Supplementary Fig. 7). Unlike Trinity, several of the *de novo* methods did not perform well in fully reconstructing transcripts within the highest expression quintiles (Supplementary Fig. 7).

Second, we assessed the accuracy of splice pattern detection. We mapped all the reconstructed transcripts (annotated or not) back to the reference genome and considered each individual intron or the combinations of introns (splicing patterns) defined by this mapping (Fig. 5c–f). We compared the number of annotated reference introns (or splicing patterns) captured by each method (Fig. 5c–f, y axis), and the number of previously unannotated introns (or extended splicing patterns) defined by each method's transcripts (Fig. 5c–f, x axis). Unannotated introns or splice patterns captured by more than one method are less likely to be false positives. In *S. pombe*, Trinity identified the largest number of reference introns (4,543) (Fig. 5c) and 1,582 unannotated introns, most of which are in putative, unannotated UTRs. Of these, 1,174 (74%) are also identified by at least one other method and thus are more likely genuine. Trinity also identifies the largest number of annotated splicing patterns in *S. pombe* (Fig. 5e). The alternative methods also report large numbers of falsely fused *S. pombe* transcripts, which are distinct transcripts encoded by adjacent genes that are reported as a single merged transcript by the assemblers. These contribute to the lack of sensitivity of the alternative methods.

In mouse, most methods had similarly high sensitivity for detecting individual annotated introns (Fig. 5d), but varied in detecting complete splicing patterns (Fig. 5f). Scripture identifies the most annotated splicing patterns (7,274), closely followed by Trinity (7,127). However, Scripture reports >110,000 unique splicing patterns, about tenfold more than Trinity and all other methods (each less than 10,000 unique patterns), suggesting many false positives in Scripture, and excellent precision in Trinity. Overall, relatively few of the nonannotated splicing patterns predicted by each method are supported by at least one other method (18–25%). (The notable exceptions were the particularly low fraction for Scripture (2%) and high fraction for ABYSS (66%).)

Finally, we examined the number of distinct contigs that mapped to each reference genomic locus, as well as the coverage (tiers) of reconstructed transcripts per locus. This accounts for multiple reported transcripts that represent the same region of a locus owing, for example, either to alternative splicing, captured allelic variation or enumerating transcripts with otherwise undetected sequencing errors. In *S. pombe*, Trinity reports 7,057 transcripts that map to 4,874 genes with an average coverage of 1.37 tiers per gene, similar to all the alternative

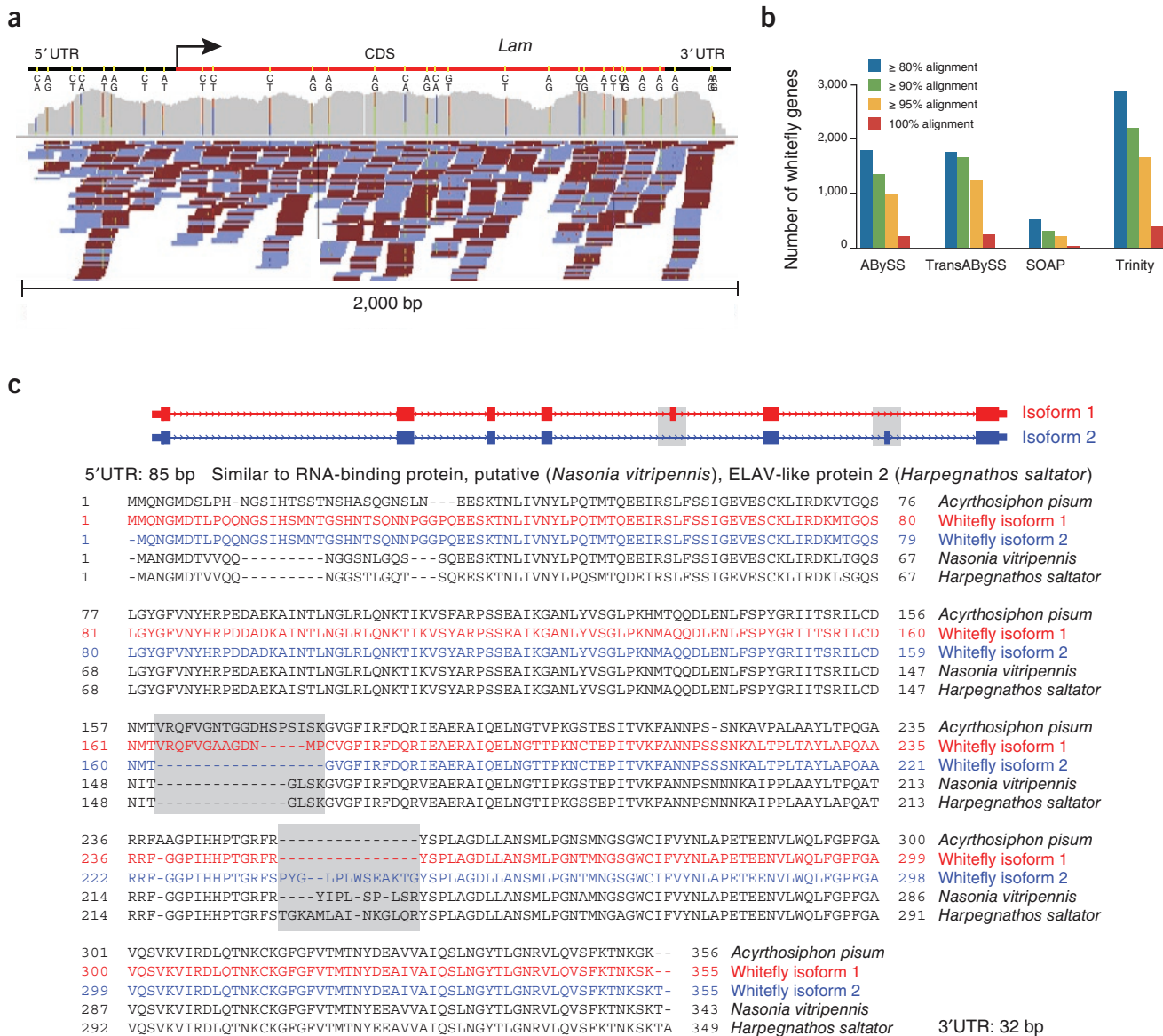


Figure 6 Trinity reconstructs polymorphic transcripts in whitefly. **(a)** Allelic variation evident from mapping RNA-Seq reads to a full-length whitefly transcript reconstructed by Trinity. At the top is a schematic of a single transcript orthologous to the *Drosophila melanogaster* Lamin gene *Lam*, identified by grouping reconstructed transcripts having allelic variants (colored yellow). Gray coverage plot shows cumulative read coverage along the transcripts. SNPs are marked with colored bars and scaled based on the relative proportions of each variant (blue: C, red: T, orange: G, green: A). Individual reads are shown below coverage plot (forward reads, blue; reverse, red). **(b)** Comparison of performance for *de novo* assembly of the whitefly transcriptome. The y axis is a count of the unique top-matching (BLASTX) uniref90 (ref. 20) protein sequences aligned Trinity transcripts across a minimal percent of their length. **(c)** Example of two alternatively spliced transcripts resolved even in the absence of a reference genome. Shown are two isoforms of an ELAV-like gene reconstructed by Trinity (gray boxes indicate alternative exons). Exon structure is determined for visualization by the *D. melanogaster* ortholog. The protein sequence alignment shows the similarity between the two whitefly isoforms and orthologous proteins from other insects, and it confirms the splice variants (gray boxes).

methods except Scripture (4.37 tiers per gene) and trans-ABySS (5.08 tiers per gene). In mouse, the performance of Trinity (31,706 contigs map to 11,334 genes, 2.05 tiers per gene on average) is similar to that of all other methods except trans-ABySS (111,000 contigs, 10,685 genes, 5.93 tiers). The large numbers of Trans-ABySS transcripts covering similar regions of loci is not reflected in the number of distinct splicing patterns, indicating that multiple similar transcript sequences are being generated at individual loci, rather than many different splice isoforms. ABySS alone, although lacking the higher sensitivity of Trans-ABySS, reports a smaller number of contigs (~1 transcript tier per locus).

De novo assembly of the whitefly transcriptome

In the absence of a sequenced genome, *de novo* assembly of RNA-Seq is the only viable option to study the transcriptomes of most organisms to date. For example, although the highly diverse class Insecta contains several key model organisms, it is not densely covered by high-quality draft genome sequences. In addition, insect transcriptomes exhibit complex alternative splicing patterns²⁸. The whitefly *B. tabaci* is one such example; the genome was not sequenced, and the RNA-Seq samples are genetically polymorphic, as they are derived from a mixture of individuals from an outbred population²⁸.

We applied Trinity to a published RNA-Seq data set from whitefly, consisting of ~21.9 million pairs of 76-base Illumina reads, sequenced using conventional non-strand-specific methods²⁹. Trinity produced 196,000 transcripts, 14,522 >1,000 base pairs, capturing allelic variants (Fig. 6a). Of those, 4,323 had top BLASTX matches ($E \leq 10^{-10}$) to 2,880 unique UniRef90 (ref. 20) protein sequences, along at least 80% of the corresponding homologous protein sequence. This number of approximately full-length Trinity-assembled transcripts is substantially higher than achieved by other *de novo* assemblers (Fig. 6b).

To assess the extent to which alternative splice forms are captured by the Trinity assembly, we aligned all pairs of contigs derived from individual graph components, and searched for evidence of at least one alternative internal exon of minimum length 21 bp and a multiple of 3. By this definition, 325 components contain at least two different isoforms. One such example (Fig. 6c) is a highly conserved ortholog to an ELAV-like protein in the ant *Harpegnathos saltator*, which is present as two different isoforms involving inclusion of two different, alternatively spliced exons.

DISCUSSION

We presented Trinity, a method for *de novo* reconstruction of the majority of full-length transcripts in a sample from RNA-Seq reads directly, across a broad range of expression levels. Trinity resolved ~99% of the initial sequencing errors, determined splice isoforms, distinguished transcripts from recently duplicated and identified allelic variants. Unlike existing short-read assembly tools initially developed for genome assembly, Trinity was designed specifically for transcriptome assembly. To this end, Trinity leverages several properties of transcriptomes in its assembly procedure: it uses transcript expression to guide the initial Inchworm transcript assembly procedure in a strand-specific manner, it partitions RNA-Seq reads into sets of disjoint transcriptional loci, and it traverses each of the transcript graphs systematically to explore the sets of transcript sequences that best represent variants resulting from alternative splicing or gene duplication by exploiting pairs of RNA-Seq reads.

Trinity's transcripts substantially enhance our annotation of the mouse and fission yeast transcriptomes. In yeast, we identified a large number of UTR extensions, antisense transcripts and novel intergenic transcripts. In mouse, we identified many novel transcripts and novel exons for reference transcripts. Trinity reconstructed many full-length transcripts from the whitefly transcriptome in the presence of substantial polymorphisms, as well as alternatively spliced variants.

Paired-reads are important to increase the distance at which Trinity can resolve ambiguities. For example, a component representing two paralogous genes (e.g., Fig. 4) or alternative isoforms can have an enormous number of possible paths, but often only very few of them represent real transcripts. Read pairs, representing longer fragments allow us to resolve differences (e.g., two pairs of single nucleotide polymorphisms (SNPs), or two different exons) that occur at that distance or below. At longer distances, there is no physical unit to support alternative paths, although similarity in expression levels could be used in the future, as well as longer reads and fragments from improved high-throughput sequencing technologies.

Evaluating the performance of transcript assemblers introduces several challenges, primarily because many transcripts, especially alternative isoforms, are not thoroughly defined as part of existing genome annotations. To address these challenges we used several complementary benchmarks. Our Oracle Set allowed us to assess sensitivity, by defining a 'gold standard' of expressed annotated transcripts present at full length. To assess our ability to reconstruct other reference transcripts, we considered the number of reference loci to which reconstructed transcripts map, and the coverage (tiers) of reconstructed transcripts per locus.

Finally, we assessed precision by considering all the reconstructed transcripts and the number of 'correct' intron boundaries and splice patterns. Each measure represents a useful benchmark, and showed that Trinity performs better than other *de novo* methods and on par with mapping-first methods depending on the organism.

Trinity is important for both genome annotation and the study of non-model organisms. For example, all but two vertebrate genomes are available only as unfinished drafts, containing sequence gaps, scaffolds that cannot be anchored to chromosomes and assembly errors³⁰. Each of these limitations hinders genome annotation and read mapping. We expect that new genomes, assembled from next-generation, high-throughput sequencing data, will be even more fragmented. Thus, high-quality *de novo* transcriptome reconstruction, as implemented in Trinity, featuring low base-error rates and the ability to capture multiple isoforms, will prove crucial to maintain acceptable levels of accuracy when characterizing genes. Finally, genomic sequences are available for only a tiny fraction of the enormous variety of organisms. Trinity provides an effective starting point to examine the transcriptomes of such species.

METHODS

Methods and any associated references are available in the online version of the paper at <http://www.nature.com/nbt/index.html>.

Accession Code. GEO (mouse data): GSE29209; SRA (fission yeast data): SRP005611. Trinity and its open source code are publicly available at <http://TrinityRNASeq.sourceforge.net>

Note: Supplementary information is available on the Nature Biotechnology website.

ACKNOWLEDGMENTS

We thank L. Gaffney for help with figure preparation, J. Bochicchio for project management, the Broad Sequencing Platform for all sequencing work, A. Papanicolaou and M. Ott for Inchworm software testing and code enhancements, and F. Ribeiro for helpful discussions regarding error pruning. The work was supported in part by a grant from the National Human Genome Research Institute (NIH 1 U54 HG03067, Lander), the Howard Hughes Medical Institute, a National Institutes of Health PIONEER award, a Burroughs Wellcome Fund–Career Award at the Scientific Interface (A.R.), the US-Israel Binational Science Foundation (N.F. and A.R.), and funds from the National Institute of Allergy and Infectious Diseases under contract no. HHSN27220090018C. M.Y. was supported by a Clore Fellowship. K.L.-T. is a recipient of the European Young Investigator Award (EYRI) funded by the European Science Foundation. A.R. is a researcher of the Merkin Foundation for Stem Cell Research at the Broad Institute.

AUTHOR CONTRIBUTIONS

M.G.G., M.Y., B.J.H., K.L.-T., N.F. and A.R. conceived and designed the study. B.J.H., M.G.G. and M.Y. developed the Inchworm, Chrysalis and Butterfly components, respectively. N.R., F.D.P., B.W.B., C.N., K.L.-T. contributed to the study's conception and execution. J.Z.L., D.A.T., X.A., L.F., R.R., I.A., N.H., A.R. and A.G. designed and performed all experiments. Q.Z., Z.C. and E.M. contributed computational analyses. M.G.G., B.J.H. and M.Y. designed, implemented and evaluated all methods. A.R., N.F., M.G.G., B.J.H. and M.Y. wrote the manuscript, with input from all authors. A.R. and N.F. contributed equally to this paper.

COMPETING FINANCIAL INTERESTS

The authors declare no competing financial interests.

Published online at <http://www.nature.com/nbt/index.html>.

Reprints and permissions information is available online at <http://www.nature.com/reprints/index.html>.

1. Birol, I. *et al.* De novo transcriptome assembly with ABYSS. *Bioinformatics* **25**, 2872–2877 (2009).
2. Trapnell, C. *et al.* Transcript assembly and quantification by RNA-Seq reveals unannotated transcripts and isoform switching during cell differentiation. *Nat. Biotechnol.* **28**, 511–515 (2010).
3. Guttman, M. *et al.* Ab initio reconstruction of cell type-specific transcriptomes in mouse reveals the conserved multi-exonic structure of lincRNAs. *Nat. Biotechnol.* **28**, 503–510 (2010).

4. Haas, B.J. & Zody, M.C. Advancing RNA-Seq analysis. *Nat. Biotechnol.* **28**, 421–423 (2010).
5. Yassour, M. *et al.* Ab initio construction of a eukaryotic transcriptome by massively parallel mRNA sequencing. *Proc. Natl. Acad. Sci. USA* **106**, 3264–3269 (2009).
6. Li, R. *et al.* SOAP2: an improved ultrafast tool for short read alignment. *Bioinformatics* **25**, 1966–1967 (2009).
7. De Bruijn, N.G. A combinatorical problem. *Koninklijke Nederlandse Akademie v. Wetenschappen* **46**, 758–764 (1946).
8. Good, I.J. Normal recurring decimals. *J. Lond. Math. Soc.* **21**, 167–169 (1946).
9. Pevzner, P.A., Tang, H. & Waterman, M.S. An Eulerian path approach to DNA fragment assembly. *Proc. Natl. Acad. Sci. USA* **98**, 9748–9753 (2001).
10. Zerbino, D.R. & Birney, E. Velvet: algorithms for de novo short read assembly using de Bruijn graphs. *Genome Res.* **18**, 821–829 (2008).
11. Butler, J. *et al.* ALLPATHS: de novo assembly of whole-genome shotgun microreads. *Genome Res.* **18**, 810–820 (2008).
12. Hertz-Fowler, C. *et al.* GeneDB: a resource for prokaryotic and eukaryotic organisms. *Nucleic Acids Res.* **32**, D339–D343 (2004).
13. Levin, J.Z. *et al.* Comprehensive comparative analysis of strand-specific RNA sequencing methods. *Nat. Methods* **7**, 709–715 (2010).
14. Parkhomchuk, D. *et al.* Transcriptome analysis by strand-specific sequencing of complementary DNA. *Nucleic Acids Res.* **37**, e123 (2009).
15. Rhind, N. *et al.* Comparative functional genomics of the fission yeasts. *Science* published online, doi:10.1126/science.1203357 (21 April 2011).
16. Wang, E.T. *et al.* Alternative isoform regulation in human tissue transcriptomes. *Nature* **456**, 470–476 (2008).
17. Wilhelm, B.T. *et al.* Dynamic repertoire of a eukaryotic transcriptome surveyed at single-nucleotide resolution. *Nature* **453**, 1239–1243 (2008).
18. Xu, Z. *et al.* Bidirectional promoters generate pervasive transcription in yeast. *Nature* **457**, 1033–1037 (2009).
19. Wu, T.D. & Watanabe, C.K. GMAP: a genomic mapping and alignment program for mRNA and EST sequences. *Bioinformatics* **21**, 1859–1875 (2005).
20. Wu, C.H. *et al.* The Universal Protein Resource (UniProt): an expanding universe of protein information. *Nucleic Acids Res.* **34**, D187–D191 (2006).
21. Wapinski, I., Pfeffer, A., Friedman, N. & Regev, A. Natural history and evolutionary principles of gene duplication in fungi. *Nature* **449**, 54–61 (2007).
22. Molnar, M. *et al.* Characterization of rec7, an early meiotic recombination gene in *Schizosaccharomyces pombe*. *Genetics* **157**, 519–532 (2001).
23. Nakamura, T., Kishida, M. & Shimoda, C. The *Schizosaccharomyces pombe* spo6+ gene encoding a nuclear protein with sequence similarity to budding yeast Dbf4 is required for meiotic second division and sporulation. *Genes Cells* **5**, 463–479 (2000).
24. Watanabe, T. *et al.* Comprehensive isolation of meiosis-specific genes identifies novel proteins and unusual non-coding transcripts in *Schizosaccharomyces pombe*. *Nucleic Acids Res.* **29**, 2327–2337 (2001).
25. Yassour, M. *et al.* Strand-specific RNA sequencing reveals extensive regulated long antisense transcripts that are conserved across yeast species. *Genome Biol.* **11**, R87 (2010).
26. Matlin, A.J., Clark, F. & Smith, C.W.J. Understanding alternative splicing: towards a cellular code. *Nat. Rev. Mol. Cell Biol.* **6**, 386–398 (2005).
27. Robertson, G. *et al.* De novo assembly and analysis of RNA-seq data. *Nat. Methods* **7**, 909–912 (2010).
28. Gravley, B.R. Alternative splicing: increasing diversity in the proteomic world. *Trends Genet.* **17**, 100–107 (2001).
29. Wang, X.-W. *et al.* De novo characterization of a whitefly transcriptome and analysis of its gene expression during development. *BMC Genomics* **11**, 400 (2010).
30. Salzberg, S.L. & Yorke, J.A. Beware of mis-assembled genomes. *Bioinformatics* **21**, 4320–4321 (2005).

ONLINE METHODS

Inchworm. Inchworm decomposes each sequence read into overlapping k -mers (default $k = 25$). Each k -mer is stored in a hash table as a key-value pair, where the key is the k -mer sequence and the value is the abundance of that k -mer in the input data set. The k -mer key is stored as a 64-bit unsigned integer with 2-bit nucleotide encoding. Likely sequencing error-containing k -mers are identified by examining k -mers that have identical $k - 1$ prefixes, differing only at their terminal nucleotide, and removing those k -mers that are <5% abundant as compared to the most highly abundant k -mer of the group. After processing the entire read set into a set of k -mers and pruning the likely error k -mers, the most frequently occurring k -mer is identified as a seed k -mer for reconstruction of draft transcript contigs. The information content of the seed k -mer is computed as Shannon's Entropy³¹, and only k -mers having entropy $H \geq 1.5$, occurring at least twice in the complete set of input reads, and not palindromic, are allowed as seed k -mers. The seed k -mer is extended at both ends in a coverage-guided manner, first from 5' to 3', followed by extension from 3' to 5'. Seed selection by Inchworm was largely inspired by similar methods implemented in the RepeatScout algorithm³². Extension from the seed is performed greedily based on the frequencies of candidate overlapping k -mers, with the single most abundant k -mer with $(k - 1)$ overlap chosen to provide a single-base extension. In the case of tied extensions, paths are recursively explored to identify the extension yielding the cumulatively maximal coverage. Extension continues until no k -mer exists in the data set to provide an extension. The sequence yielded from the bidirectional seed k -mer extension is reported as a draft transcript contig, and the set of overlapping k -mers comprising the contig are removed from the hash table. The entire cycle of seed selection and bidirectional k -mer extension continues until all k -mers in the hash table have been exhausted.

In strand-specific mode (default), k -mers are derived from only the sense strand of the RNA-Seq read. Double-stranded mode, used with non-strand-specific RNA-Seq data involves several modifications: both the sense and the reverse-complemented read sequence are parsed into overlapping k -mers; during Inchworm contig extension, a k -mer chosen to extend a given path has the reverse-complemented k -mer sequence disabled for further k -mer extensions; and when an Inchworm contig is reported at the end of one iteration of contig assembly, both the sense and reverse-complemented k -mers are removed from the k -mer dictionary.

Only Inchworm contigs with an average k -mer coverage of 2 and length at least 48 ($2^*(k - 1)$, $k = 25$), the minimal contig length required to capture variation anchored by $(k - 1)$ at each terminus, are used by Chrysalis, as described below.

Chrysalis. To convert the linear contigs into a proper de Bruijn graph, Chrysalis first builds a $k - 1$ -mer lookup table and recursively pools contigs that share sequences (excluding low-complexity sequence, as above in Inchworm) into components, given that there are reads that span across a potential junction (the 'welds') and extend perfect matches by $(k - 1)/2$ bases on each side. The number of welds must exceed 0.04 times the average $k - 1$ -mer coverage of each contig (twice the sequencing error rate in a read, the upper bound of which we estimate at ~2%), as computed by Inchworm. In addition, the $k - 1$ -mer coverage of one contig cannot exceed the coverage of the other by a factor of 100 (empirically determined). Next, Chrysalis processes each component individually and computes a de Bruijn graph from the linear inchworm contigs. The reads are then mapped to components by selecting the component that shares the most $k - 1$ -mers with the read, with a single $k - 1$ -mer being sufficient for assignment. Chrysalis also counts all k -mers and stores them as 'edge weight' to indicate their support in the read set. Components with less than a minimum number of nodes are discarded (a configurable parameter that defaults to an empirically determined value of 300 – $(k - 1) = 276$).

Butterfly. The input to butterfly is a de Bruijn graph component as built by Chrysalis. First, Butterfly trims edges in the de Bruijn graph. It uses two criteria. (1) We reasoned that if there is a node with several outgoing edges, such that one of them has a much smaller read support than the total outgoing reads (less than 5%), then it probably represents a sequencing error or a variant with very low expression (Supplementary Fig. 8a). (2) If the outgoing edge has less than 2% support from the total incoming reads, then it is more likely a spurious transcript extension (Supplementary Fig. 8b). Outgoing or incoming edges that fail according to one of these criteria are removed (both these numbers are parameters to the program, and can be changed for specific requirements).

Second, Butterfly transforms the modified graph into a weighted sequence graph, where each node is a sequence, rather than an individual k -mer providing a single-base path extension as in the de Bruijn graph. In this step, Butterfly gener-

ates a compact graph—the set of paths in the compacted graph is identical to that of the original de Bruijn graph. As a result, linear paths will be compacted into a single node, and polymorphisms will be minimized. The weight on each edge of the modified graph corresponds to the number of reads supporting the edge in the original de Bruijn graph. For each compound node, we compute the average coverage, which corresponds to the weights of the original edges that made up the sequence divided by the length of the node.

We then repeat the trimming step, except that when examining compound nodes of length >1, we also use the node coverage as a measure of opposite flow in the second criterion. These two steps (trimming and graph compaction) are reiterated until convergence. The resulting graph represents possible transcripts as paths through the graph.

Finally, Butterfly uses read sequences, read-pairings and Chrysalis' read mappings to the graph to select the paths that are best supported by read sequences. The goal is to look for paths with physical evidence for contiguity, by either reads or read pairings. To do so, we first represent all the reads that contributed to the de Bruijn graph by the list of the nodes that they traverse. We then use a dynamic programming algorithm for finding supported path prefixes. The procedure is initialized with source nodes in the graphs (one without incoming edges), and at each step one path prefix is extended by an additional node.

When extending a path prefix that ends at node n , we consider all outgoing edges from n , and evaluate the support for the extension. By construction, each edge in the graph is supported by reads. We however, further require that the last L nucleotides of the path be supported by reads. We define a path as L -supported at coverage c if at each extension of this path, we have at least c reads supporting the L nucleotide suffix of this path (Supplementary Fig. 8c). A read supports a path fragment either if it contains that fragment as a subsequence, or in the case of paired-reads, if the fragment lies on all paths from nodes that correspond to the first sequence mate to the second sequence mate. In addition, to avoid combinatorial explosion because of small variations (most likely caused by sequence errors), once we extend a path prefix, we examine other paths ending at the same node, and merge the new path with previous path prefix ending at the same node if the two are >95% identical.

In the results here we used $L = 250$ and $c = 2$. The requirement for 250-supported paths emerges from the expected insert size of our library, as we do not expect to have support for a longer suffix if our read pairs (derived from a single fragment) do not span that far. We note that the resolution of ambiguities, which includes alternative splicing and allelic variation, is limited to the insert size of the read pairs, or the read lengths for unpaired data. Although this program can in theory exponential in size, in practice its cost is defined by the number of supported paths.

Yeast and mouse cell growth conditions. We used the *S. pombe* strain SPY73 975h+ and dendritic cells isolated from C57BL/6J mice. Details of cell isolation and growth conditions are in the Supplementary Methods.

RNA isolation for yeast samples. Total yeast RNA was isolated using Qiagen RNeasy kit following manufacturers' protocol for mechanical lysis using 0.5 mm zirconia/silica beads (Biospec). PolyA⁺ RNA was isolated from total RNA using Poly(A) purist kit (Ambion) or Dynabeads mRNA purification kit (Invitrogen). Total RNA and polyA⁺ RNA were treated with Turbo DNA-free (Ambion), as described. The integrity of the RNA was confirmed using the Agilent 2100 Bioanalyzer and quantified using RNA Quant-It assay for the Qubit Fluorometer (Invitrogen).

RNA preparation for mouse RNA. Dendritic cells were lysed using QIAzol reagent and total RNA was extracted with the miRNeasy kit's procedure (Qiagen), sample quality was controlled on a 2100 Bioanalyzer (Agilent).

RNA-Seq library preparation. For the mouse dendritic cell sample, we created a dUTP second strand library starting from 200 ng of Turbo DNase treated and poly(A)⁺ RNA using a previously described method¹⁴ except that we fragmented RNA in 1× fragmentation buffer (Affymetrix) at 80 °C for 4 min, purified and concentrated it to 6 µl after ethanol precipitation. For the *S. pombe* samples, we prepared dUTP second-strand libraries similarly, with the following additional modifications. We added an index (8-base barcode) to each library to enable pooling of these libraries (S. Fisher, Broad Institute, personal communication). In addition, the adaptor ligation step was done with 1.2 µl of index adaptor mix and 4,000 cohesive end units of T4 DNA Ligase (New England Biolabs) overnight at 16 °C in a final volume of 20 µl. Finally, we generated libraries with an insert size ranging from 225 to 425 bp.



RNA-Seq library sequencing. We sequenced all the cDNA libraries with an Illumina Genome Analyzer IIx. We pooled the four *S. pombe* libraries together with four other indexed libraries and sequenced them using eight lanes of 76-base paired reads. We sequenced the mouse library using two lanes of 76-base paired reads.

Defining empirical limits of full-length transcript reconstruction. Inchworm was used to construct a *k*-mer dictionary based on the input reads as described above. Reference protein-coding sequences were examined by searching for each overlapping *k*-mer sequence in the dictionary. Reference protein-coding sequences lacking at least one *k*-mer in the Inchworm *k*-mer graph were classified as inaccessible for full-length reconstruction by means of the *k*-mer graph method. Those reference sequences fully represented within the *k*-mer dictionary were included in the Oracle Set.

Finding paralogous genes in mouse. To determine paralogous transcripts, we aligned all isoforms of all genes present in the Oracle Set against each other, using the alignment program *Satsuma*³³. We required alignments to be longer than half of the shorter of both sequences and at sequence identity of 70% and up. If at least one pair of transcripts from two genes met the criteria, we called both genes paralogous.

Short-read spliced alignments and transcript reconstructions using Cufflinks and Scripture. The *S. pombe* genome was obtained from the Sanger Institute (http://www.sanger.ac.uk/Projects/S_pombe/download.shtml). The mouse genome version 9 was obtained from the UCSC mouse genome browser gateway (<http://genome.ucsc.edu/cgi-bin/hgGateway?db=mm9>). Left and right fragment reads were separately aligned to the genomes using TopHat (version 1.1.4)³⁴ with mouse RNA-Seq reads, and BLAT with *S. pombe* RNA-Seq reads; the BLAT short-read alignment pipeline is provided at http://inchworm.sourceforge.net/blat_short_read_alignment.html. We found BLAT to provide more accurate short-read alignment with *S. pombe*, with TopHat lacking sensitive detection of the very short introns in *S. pombe*. In addition, both Scripture and Cufflinks demonstrated better performance using the BLAT alignments for *S. pombe* as compared to the TopHat alignments (Supplementary Fig. 9a). Conversely, performance of Scripture and Cufflinks using TopHat alignments in mouse exceeded that using BLAT alignments (Supplementary Fig. 9b). Hence, for evaluation purposes, we leveraged BLAT short-read spliced alignments in *S. pombe* and TopHat alignments in mouse.

BLAT alignments of short reads to the *S. pombe* genome were performed using the pipeline described above with the following settings: maximum intron length set to 500 bases, maximum distance between read pairs of 500, and only the single best alignment was reported per read. TopHat alignments to the mouse genome were performed using the following parameters: minimum intron length of 50 bases, maximum intron of 100 kb and mate inner distance set to 300 bases. Transcribed strand information was assigned to the individual reads based on knowledge of the fragment type (left or right) and the aligned strand of the genome. Both Cufflinks (version 0.9.3)² and Scripture³ (version VPaperR3, obtained from Scripture author Manuel Garber) were executed on these alignments.

Evaluation of published *de novo* methods. Illumina reads were *de novo* assembled using ABYSS¹ (version 1.2.1), SOAPdenovo⁶ (version 1.04) or Trans-ABYSS²⁷. Command-line parameters used with ABYSS were “abyss-pe k=25 E=0 n=10 in=‘left.fa right.fa’”, using a *k*-mer length of 25. Likewise, a 25-mer length was used with SOAPdenovo along with other default parameters. Trans-ABYSS²⁷ was run on mouse and *S. pombe* using a set of *k*-mers including 26, 31, 36, 41 and 46 followed by merging the results by running the first stage of the trans-ABYSS analysis pipeline. In the case of whitefly, all *k*-mers from 26 through 46 were used so as to maximize sensitivity given the smaller input number of reads.

Comparisons to reference transcripts. Current gene annotations for *S. pombe* were downloaded as file ‘pombe_290110.gff’ from GeneDB (<http://old.genedb.org/genedb/pombe/>). Ref-Seq transcript gene annotations were downloaded for mouse at the UCSC mouse genome browser gateway (<http://genome.ucsc.edu/cgi-bin/hgGateway?db=mm9>) in BED format. Protein coding nucleotide sequences were extracted from the genome sequences based on the gene annotations using custom PERL scripts. The mouse reference coding sequences were further distilled to remove entirely identical sequences corresponding to isoforms encoding identical proteins and paralogous sequences: the original 19,947 genes encoding 23,881 transcripts were reduced to 19,857 genes encoding 22,717 non-identical coding transcripts.

Reconstructed transcript sequences (by *de novo* assembly, Scripture or Cufflinks) were mapped to the reference coding sequences using BLAT³⁵. Full-length reference annotation mappings were defined as having at least 95% sequence identity covering the entire reference coding sequence and containing at most 5% insertions or deletions (cumulative gap content). In evaluating methods that leverage the strand-specific data (Trinity and Cufflinks), proper sense-strand mapping of sequences was required. Transcripts reconstructed by the alternative methods (Scripture, ABYSS and SOAPdenovo) were allowed to map to either strand. Fusion transcripts were identified as individual reconstructed transcripts that mapped as full-length to multiple reference coding sequences and lacked overlap among the matching regions within the reconstructed transcript. One-to-one mappings were required between reconstructed transcripts and reference transcripts, including alternatively spliced isoforms, with the exception of fusion transcripts.

Analysis of alignment-inferred introns and splicing patterns from reconstructed transcripts. Reconstructed transcripts were mapped to genome sequences using GMAP, reporting only the single top-scoring alignment per sequence. Individual introns and complete splicing patterns were extracted from each of the alignments and compared to reference annotations using custom PERL scripts. Unique introns (missing from the reference annotations) were required to contain consensus dinucleotide splice sites (GT or GC donors and AG acceptors).

Locus coverage (tiering) by reconstructed transcripts. The BLAT alignments between reference coding sequences (loci) and reconstructed transcripts described above were organized into locus-level coverage tiers as follows. Given a set of different reconstructed transcripts that have a best match to a reference sequence, the first match is selected and applied to that reference contig at the first coverage tier. The remaining matches are then examined for placement in the first tier. If a subsequent reference-matching region in common between two matches exceeds 30% of the shorter match length, then this subsequent match is propagated to the next highest tier lacking such restrictive match overlap. Tier placement continues until all matches are placed. The maximal tier level defines the locus-level coverage for that reference sequence and can be at most equal to the number of reconstructed transcripts mapped to that locus. Strand-specific transcript reconstructions were tiered in a strand-specific manner (as in the case of Trinity and Cufflinks). In the case of a highly fragmented transcriptome assembly, it is possible for many reconstructed transcripts to populate the first tier yielding a coverage of 1. In the case of alternatively spliced isoforms or redundant transcript generation at a given locus, the coverage value will exceed 1.

Running Trinity on data sets of varying read depth. We randomly subsampled pairs in the mouse data set to generate such subsets. Inchworm and Chrysalis were run on a server with 256 GB of RAM, Butterfly on a server (*load sharing facility* (LSF)) farm in parallel. Wall-clock run times are: ~17 h (10 M pair set), ~36 h (30 M pair set), and ~60 h (full 50 M pair set). All experiments were performed with Trinity using parameters: minimum contig length of 100 bases and average fragment length of 300 bases.

Computing gene expression values from aligned RNA-Seq reads. The aligned reads (by TopHat in the case of mouse leveraging the full 52.6M read pairs, and by BLAT in the case of *S. pombe* leveraging the 50 M read pairs) were used for computing gene (and other feature) expression values. The number of fragments mapped to segments (exons) of a genome-mapped feature were tallied based on overlap of the segment’s coordinates by either read from a sequenced fragment, counting fragments as opposed to counting individual reads. Expression was computed as the normalized value of fragments per kilobase of feature sequence per million fragments mapped, or FPKM². Calculations were performed using custom PERL scripts. Genes were defined as ‘expressed’ if observed to have expression values of at least 0.5 FPKM, and these genes were divided into expression quintiles at 5% intervals for purposes of analysis.

31. Shannon, C.E. Prediction and entropy of printed English. *Bell Syst. Tech. J.* **30**, 50–64 (1951).
32. Price, A.L., Jones, N.C. & Pevzner, P.A. De novo identification of repeat families in large genomes. *Bioinformatics* **21** Suppl 1, i351–i358 (2005).
33. Grabherr, M.G. et al. Genome-wide synteny through highly sensitive sequence alignment: Satsuma. *Bioinformatics* **26**, 1145–1151 (2010).
34. Trapnell, C., Pachter, L. & Salzberg, S.L. TopHat: discovering splice junctions with RNA-Seq. *Bioinformatics* **25**, 1105–1111 (2009).
35. Kent, W.J. BLAT—the BLAST-like alignment tool. *Genome Res.* **12**, 656–664 (2002).